Pre-Clinical Research Report

Journal of INTERNATIONAL MEDICAL RESEARCH

Journal of International Medical Research
2019, Vol. 47(3) 1264–1278

DOI: 10.1177/0300060518814333
journals.sagepub.com/home/imr
SAGE

Spherical silica nanoparticles promote malignant transformation of BEAS-2B cells by stromal cell-derived factor-1α (SDF-1α)

Chong Guo[1,2], Ding-Yun You[3], Huan Li[1], Xiao-Yu Tuo[2] and Zi-Jie Liu[1,2]

Abstract

Objective: This study aimed to examine the role of spherical silica nanoparticles (SiNPs) on human bronchial epithelial (BEAS-2B) cells through inflammation.

Methods: Human mononuclear (THP-1) cells and BEAS-2B cells were co-cultured in transwell chambers and treated with 800 mmol/L benzo[*a*]pyrene-7, 8-dihydrodiol-9, 10-epoxide (BPDE) and 12.5 μg/mL SiNPs for 24 hours. For controls, cells were treated with BPDE alone. Subcutaneous tumorigenicity and epithelial-mesenchymal transition (EMT) of BEAS-2B cells were measured. The cells were blocked with a stromal cell-derived factor-1α (SDF-1α)-specific antibody. EMT was analyzed in cells treated with 800 mmol/L BPDE and 12.5 μg/mL SiNPs relative to matched control cells and xenografts *in vivo*. Serum SDF-1α levels were measured in 23 patients with lung adenocarcinoma in Xuanwei, in 25 with lung adenocarcinoma outside Xuanwei, and in 22 with benign pulmonary lesions in Xuanwei.

Results: SiNPs significantly promoted tumorigenesis and EMT, induced the release of SDF-1α, and activated AKT (ser473) in BEAS-2B cells. EMT and phosphorylated AKT (ser473) and glycogen synthase kinase-3β levels were decreased when blocked by SDF-1α antibody in BEAS-2B cells. SDF-1α was mainly secreted by THP-1 cells.

Conclusion: SiNPs combined with BPDE promote EMT of BEAS-2B cells via the AKT pathway by inducing release of SDF-1α from THP-1 cells.

[1]Department of Laboratory Medicine, First Affiliated Hospital of Kunming Medical University, Kunming, Yunnan, China
[2]Yunnan Key Laboratory of Laboratory Medicine, Kunming, Yunnan, China
[3]School of Public Health, Kunming Medical University, Kunming, Yunnan, China

Corresponding author:
Zi-Jie Liu, Department of Laboratory Medicine, The First Affiliated Hospital of Kunming Medica, University; Yunnan Key Laboratory of Laboratory Medicine, Kunming, #295 Xichang Road, Kunming City, Yunnan Province, China.
Email: redjacky502@aliyun.com

Keywords
Benzopyrene, silica nanoparticles, inflammation, epithelial-mesenchymal transition, lung cancer, stromal cell-derived factor-1α, AKT pathway

Date received: 24 July 2018; accepted: 29 October 2018

Introduction

Xuanwei City in Yunnan Province has a particularly high incidence of lung cancer. The incidence of lung cancer is 20 to 30 times higher than in other regions of China, and even ranks first in the world in non-smoking women.[1] Epidemiological studies have shown that the high incidence of lung cancer in Xuanwei has a significant correlation with locally produced bituminous coal.[2] Polycyclic aromatic hydrocarbons (PAHs) can be generated after combustion of bituminous coal. The carcinogenic effects of PAHs, represented by benzo[a]anthracene, have been supported by most studies, and their metabolites can directly bind to DNA to form DNA adducts, thereby causing DNA damage.[3,4] However, the concentration of PAHs in the air is not entirely consistent with the incidence of lung cancer in Xuanwei. Additionally, PAHs are not specific to bituminous coal in Xuanwei. Therefore, the theory of carcinogenesis of organic carcinogens, represented by benzopyrene, is not sufficient to explain the high incidence of lung cancer in Xuanwei. However, the burning of Xuanwei bituminous coal produces not only PAHs, but also dust. Geology and chemistry studies have shown that the incidence of lung cancer in Xuanwei is also correlated with the high content of silica nanoparticles in the C1 coal seam.[5,6] The spatial distribution of lung cancer mortality coincides with the distribution of the C1 coal seam, and the mortality rate is higher in corresponding production areas.[6] Crystalline silica is a carcinogen, but silica nanoparticles in Xuanwei bituminous coal are amorphous, (i.e., mainly irregular and spherical).[7] At present, amorphous silica is believed to be relatively safe. Therefore, explaining the high incidence of lung cancer in Xuanwei is difficult just by the theory of direct carcinogenesis of amorphous silica nanoparticles.

However, increasing evidence has shown that silica nanoparticles can cause inflammation.[8] Inflammation is considered to be an important cause of the onset of some tumors. Spherical silica nanoparticles (SiNPs) are the smoothest type of amorphous silica. Consequently, they are less likely to be eliminated through the respiratory tract than irregular silica nanoparticles, and more likely to cause chronic inflammation. In the chronic inflammatory environment, DNA damage induced by benzopyrene in Xuanwei bituminous coal is more likely to induce tumorigenesis and development of tumors. Therefore, we speculate that organic compounds, represented by benzopyrene, and SiNPs released from Xuanwei bituminous coal, may have a combined effect on tumorigenesis of lung cancer in Xuanwei. Inflammatory cells and immune regulation mediate the tumor microenvironment, affecting tumor progression through the specific phenotype of the host immune response.[9] Lens epithelial cells can be changed into interstitial like cells in a collagen gel, which leads to epithelial-mesenchymal transition (EMT).[10] EMT occurs in the tumor microenvironment and is regulated by inflammatory cells and cytokines. EMT is also an

important factor in the occurrence and metastasis of tumors. Stromal cell-derived factor-1α (SDF-1α) is one of the major chemokines that is consistently overexpressed in most solid tumors, where it contributes to carcinogenesis and promotes angiogenesis and recruitment of cells to the tumor microenvironment.[11] SDF-1α is also a constitutively expressed and inducible chemokine that plays a fundamental role in embryonic development, organ homeostasis, angiogenesis, and immune system modulation.[12]

This study aimed to examine the role of SiNPs in EMT of human bronchial epithelial cells and human mononuclear cells through inflammation. Proliferation and expression of EMT markers of BEAS-2B cells were detected. To study the mechanism, cytokine chips and an enzyme-linked immunosorbent assay (ELISA) were used to screen out the differentially expressed cytokines and explore the role of cytokines *in vitro* and *in vivo*.

Materials and methods

Ethics

The study was approved by the Ethics Committee of Kunming Medical University, China (No. KMMC2017056). Animal work was performed in compliance with the guidelines established by the Kunming Medical University Institutional Animal Care and Use Committee (No. KMIACU2017043). All subjects signed informed consents.

Blood samples

Blood samples were collected from the First and Third Affiliated Hospitals of Kunming Medical University after clinical examination from November 2017 to May 2018. The criteria for inclusion of patients with lung adenocarcinoma from Xuanwei were as follows: patients lived in Xuanwei, Yunnan, and had lived there for longer than 15 years; and the patients were diagnosed with lung adenocarcinoma by pathology and had received no systemic treatment. The criteria for inclusion of non-Xuanwei patients with lung adenocarcinoma were as follows: patients lived outside of Xuanwei, Yunnan, and had not previously lived in Xuanwei; and patients were diagnosed with lung adenocarcinoma by pathology and had received no systemic treatment. The inclusion criteria for patients with benign pulmonary lesions in Xuanwei were as follows: patients lived in Xuanwei, Yunnan, and had lived there for longer than 15 years; lung cancer was clearly excluded and other pulmonary diseases were diagnosed; and there were no bacterial and viral pulmonary infections. A total of 70 patients were enrolled in this study, including 23 patients with lung adenocarcinoma in Xuanwei (8 men and 15 women), 25 patients with lung adenocarcinoma outside of Xuanwei, Yunnan (13 men and 12 women), and 22 patients with benign pulmonary lesions in Xuanwei (9 men and 13 women). The serum of patients was collected after clinical tests and stored in liquid nitrogen.

Cell lines and cell culture

Human bronchial epithelial cells (BEAS-2B) (KCB 200922YJ), human mononuclear cells (THP-1) (KCB 200549YJ), and LHC-9 medium were purchased from Kunming Institute of Zoology, Chinese Academy of Sciences. BEAS-2B cells were cultured in LHC-9 medium supplemented with 1% penicillin and streptomycin (Thermo Fisher Scientific, Rockford, IL, USA). THP-1 cells were cultured in RPMI1640 medium (HyClone, Logan UT, USA) with 10% fetal bovine serum (HyClone) and 1% penicillin and streptomycin. The cells were

routinely cultured at 37°C in a humidified atmosphere with 5% CO_2.

Cell viability

The Cell Counting Kit-8 (Dojindo Molecular Technologies, Inc., Kumamoto, Japan) was used to detect the viability of THP-1 and BEAS-2B cells. The cells were exposed to various concentrations of benzo [*a*]pyrene-7, 8-dihydrodiol-9, 10-epoxide (BPDE) (0, 200, 400, 800, and 1000 mmol/L) or SiNPs (0, 3.125, 6.25, 12.5, and 25.0 μg/mL) for 48 hours. After replacing the RPMI 1640 medium, 10 μL of cholecystokinin-8 reagent (Dojindo Molecular Technologies, Inc.) was added to each well, and the 96-well plate was incubated at 37°C for 1.5 hours. The absorbance was measured at 450 nm by a microplate reader (Thermo Fisher Scientific). All of the experiments were performed in triplicate.

Xenografts

BEAS-2B cells were cultured for three generations and 0.2 mL of a 1×10^6 cell/mL suspension was inoculated subcutaneously into the right flank of male BALB/c nude mice (Animal Experiment Center of Kunming Medical University, Yunnan, China). The experimental and control groups each contained three nude mice. Measurement of tumor volume began when the tumors were visible to the naked eye and was conducted every 2 days thereafter. The tumor volume was calculated as follows: V (mm^3) = A (mm) × B2 (mm^2) × 0.5 (A, length; B, width).[13] The tumor growth curve was plotted against time. After 25 days, the mice were sacrificed and the tumor tissues were measured and stored at −80°C.

Analysis of cytokines

BEAS-2B cells were primed with 800 nmol/L BPDE for 12 hours and THP-1 cells were starved in a reduction medium based on RPMI 1640 medium for 12 hours. THP-1 cells were then re-suspended in LHC-9 medium and added to the upper chamber, and cultured with or without 12.5 μg/mL SiNPS for 48 hours. The culture supernatant was collected and centrifuged at 5000 × g for 10 minutes. The release of cytokines and chemokines was analyzed using a Human XL Proteome Profiler™ Array, in conjunction with the Cytokine Array Kit (ARY022B; R&D Systems, Minneapolis, MN, USA). Export signal values and the average signals (pixel density) of the pairs of duplicate spots were determined and compared with corresponding signals on different arrays to determine the relative change between the control and treated groups.

Immunohistochemistry and immunocytochemistry

Paraffin-embedded tissue sections were deparaffinized, dehydrated, and boiled for 15 minutes in 0.01 M phosphate buffer (pH, 7.2). BEAS-2B cells were fixed on slides for further use. Endogenous peroxidases were blocked by incubation in 3% hydrogen peroxide for 30 minutes. Non-specific binding sites were blocked with 10% normal goat serum (Boster, Wuhan, China) for 30 minutes at 37°C, after which the tissue samples were incubated at 4°C overnight with the following primary antibodies: anti-E-cadherin antibody (ab76055; Abcam, Cambridge, MA, USA), anti-vimentin antibody (ab92547; Abcam), anti-pan cytokeratin antibody (ab215838; Abcam), anti-fibronectin antibody (30339; ProMab, Richmond, CA, USA), anti-AKT (21054-1; SAB, Nanjing, China), anti-p-AKT(Ser473)

(ab81283; Abcam), anti-GSK-3β (ab93926, Abcam), anti-p-GSK-3β (Ser9) (5558; Cell Signaling Technology, Danvers, MA, USA), anti-β-actin (sc-47778; Santa Cruz Biotechnology, Dallas, TX, USA). The tissue samples were then incubated with secondary peroxidase-conjugated antibodies (5210-0191, 5210-0176; KPL, Milford, MA, USA) for 30 minutes at 37°C and developed with 2% 3,3-diaminobenzidine tetrachloride (MaiXin, Fuzhou, China) until the desired brown product was obtained. Finally, the sections were counterstained with hematoxylin (MaiXin). The negative control group went through the same steps as described above, except for replacing the primary antibody with phosphate-buffered saline. All slides were observed under a BX53 light microscope (Olympus, Tokyo, Japan). For immunocytochemistry, BEAS-2B cells co-cultured with THP-1 cells (after treatment with 800 nmol/L BPDE and 12.5 μg/mL SiNPs) were fixed on slides with 4% paraformaldehyde and air-dried. The subsequent steps were the same as those described for immunohistochemistry.

Relative quantitative real-time polymerase chain reaction

Total RNA was reverse transcribed using the RevertAid^{TM} H Minus First Strand cDNA Synthesis Kit (Fermentas; Thermo Fisher Scientific). The abundance of mRNA was determined on an HT7900Real-Time PCR system (Applied Biosystems, Foster City, CA, USA) using SYBR Green PCR Master Mix (Applied Biosystems), and each sample was measured three times. Relative expression levels were calculated according to the comparative threshold cycle method ($2^{-\Delta\Delta Ct}$) using glyceraldehyde-3-phosphate dehydrogenase as an endogenous control gene.[14] Primers for expression analysis were synthesized by Sangon Biotech (Shanghai, China). The primers for SDF-1α were 5′-AGGTCCGAAAACACTGTGA GT-3′ and 5′-AGCAAGCGGTTCTTCCCTTC-3′, and the primers for glyceraldehyde-3-phosphate dehydrogenase were 5′-GG AGCGAGATCCCTCCAAAAT-3′ and 5′-GGCTGTTGTCATACTTCTCATGG-3′.

Western blot analysis

Total protein of BEAS-2B cells was extracted using the Total Protein Extraction Kit (ProMab). The total protein concentration was measured using the Bio-Rad DC Protein Assay kit (Bio-Rad, Hercules, USA). An aliquot comprising 20 μg of total protein was used for sodium dodecyl sulfate-polyacrylamide gel electrophoresis. The separated protein bands were transferred to a polyvinylidene difluoride membrane after blocking with defatted milk at 37°C for 2 hours, and incubated individually with anti-AKT, anti-p-AKT (Ser473), anti-glycogen synthase kinase (GSK)-3β, anti-p-GSK-3β (Ser9), and anti-β-actin antibodies at 4°C overnight (see the Immunohistochemistry and immunocytochemistry section above). The antibody-bound polyvinylidene difluoride membrane was rinsed with Tris-buffered saline supplemented with 0.1% Tween 20 (3×5 minutes) and incubated with horseradish peroxidase-labeled secondary antibody (KPL) for 1 hour. The secondary antibody was discarded, and the membrane was rinsed with Tris-buffered saline supplemented with 0.1% Tween 20 (3×5 minutes). The proteins were detected using enhanced chemiluminescence (NCI4106; Pierce, Waltham, MA, USA) in conjunction with Bio-Rad Electrophoresis Documentation software (Gel Doc 1000; Bio-Rad) and Quantity One Version 4.5.0 (Bio-Rad). The proteins were quantified and expressed as their ratio to β-actin.

ELISA

Cell culture supernatants or patients' serum samples were analyzed using a commercially available ELISA kit for SDF-1α (Xinbosheng Biological Technology, Shenzhen, China). After the kit was balanced at room temperature, 100 μL of blank control, specimen, and standard were added to individual wells of a 96-well plate, incubated for 90 minutes at 37°C, and washed five times with washing solution. Subsequently, 100 μL of the biotinylated antibody working fluid was added, incubated for 60 minutes at 37°C, and washed five times. After 100 μL of enzyme binding solution was added, the plate was incubated for 30 minutes at 37°C in the dark. After washing five times, 100 μL of tetramethylbenzidine was added to each well, and the plate was incubated in the dark for 15 minutes at 37°C. Finally, 100 μL of stopping buffer was added to each well. After mixing, the OD_{450} value was immediately measured in a Multiskan sky microplate reader (Thermo Fisher Scientific).

Neutralization of SDF-1α

BEAS-2 cells were treated with 3 ng/mL rabbit anti-SDF-1α antibody (ab9797; Abcam) relative to immunoglobulin G control (ab172730; Abcam,). BEAS-2 and THP-1 cells were then co-cultured in transwell chambers and treated with 800 mmol/L BPDE and 12.5 μg/mL SiNPs for 48 hours. EMT was analyzed in cells or xenograft tissues.

Statistical analysis

Statistical analysis was performed using SPSS software version 17.0 (SPSS Inc., Chicago, IL, USA). Measurement data with a normal distribution are expressed as mean ± standard error of the mean, and data with a partial distribution are shown as the median, minimum, and maximum. For variables with two groups, the *t*-test was used for parametric analysis and the Mann–Whitney test was used for non-parametric analysis. Differences with p values < 0.05 were considered statistically significant.

Results

Study population

Characteristics of the study population are shown in Table 1.

SiNPs promote EMT of BEAS-2B cells in vitro and in vivo

SiNPs were analyzed by scanning electron microscopy at the Advanced Analysis and Measurement Center of Yunnan University (Kunming, Yunnan, China). The particles were spherical with a uniform size of approximately 30–50 nm, with good dispersion and no obvious agglomeration (Figure 1a). BEAS-2B and THP-1 cells were treated with different concentrations of BPDE and SiNPs and cell viability was then analyzed. Only 25 μg/mL SiNPs showed a significant inhibition on growth of BEAS-2B cells ($p < 0.05$ versus 12 μg/mL) (Figure 1b, c). Therefore, 12.5 μg/mL SiNPs and 800 nmol/L BPDE were chosen for the subsequent study. To examine whether SiNPs can enhance EMT of BEAS-2B cells after priming with BPDE, immunocytochemistry was used to detect EMT markers of BEAS-2B cells. We found that cytokeratin and E-cadherin expression in BEAS-2B cells was lower, while fibronectin and vimentin expression was higher in cells with treatment of BPDE and SiNPs compared with cells treated with BPDE alone (controls) (Figure 2a). BEAS-2B cells were then inoculated subcutaneously into nude mice. Visible lumps were found after approximately 5 days (Figure 2b). Tumor

Table 1. Characteristics of the study population (n = 70).

	Lung adenocarcinoma in Xuanwei (n = 23)	Lung adenocarcinoma outside of Xuanwei in Yunnan (n = 25)	Benign pulmonary lesions in Xuanwei (n = 22)	p value
Sex				
Male	10	12	12	0.757
Female	13	13	10	
Age (years)				
<50	9	5	12	0.001
≥50 and ≤60	12	5	6	
>60	2	15	4	
Smoking status				
Former/current	7	8	10	0.512
Never	16	17	12	
Stage of TNM				
IA, IB	14	10	/	0.272[$]
IIA, IIB	4	9	/	
IIIA, IV	5	6	/	

[$]Patients with lung adenocarcinoma in Xuanwei were compared with those with lung adenocarcinoma outside of Xuanwei in Yunnan

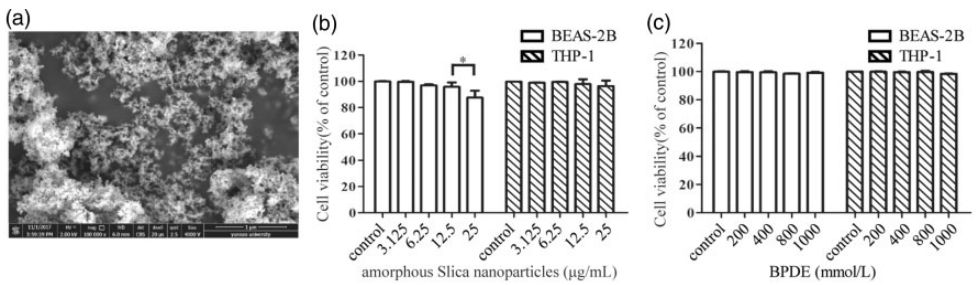

Figure 1. (a) Representative electron microscopic image of amorphous silica nanoparticles. (b) Effect of amorphous silica nanoparticles on the viability of BEAS-2B and THP-1 cells at different concentrations and (c) B. Effect of BPDE on the viability of BEAS-2B and THP-1 cells at different concentrations.
BPDE: benzo[a]pyrene-7, 8-dihydrodiol-9, 10-epoxide. *$p < 0.05$.

tissues were stained by hematoxylin–eosin staining and identified by two pathologists (Figure 2c). The tumor cells had a solid shape, were localized in adenoids, and had marked pleomorphism. The nucleus was heterogeneous and deeply stained. The chromatin was thick and the cytoplasm was basophilic. Mucous vacuoles and signet ring-like changes were found in some cells. Adenocarcinoma-like changes were identified by the two pathologists. Cytokeratin and E-cadherin expression was lower, but fibronectin and vimentin expression was higher compared with the control group of BPDE alone (Figure 2c). These results suggested that SiNPs combined with BPDE could promote tumorigenesis and EMT of BEAS-2B cells *in vitro* and *in vivo*.

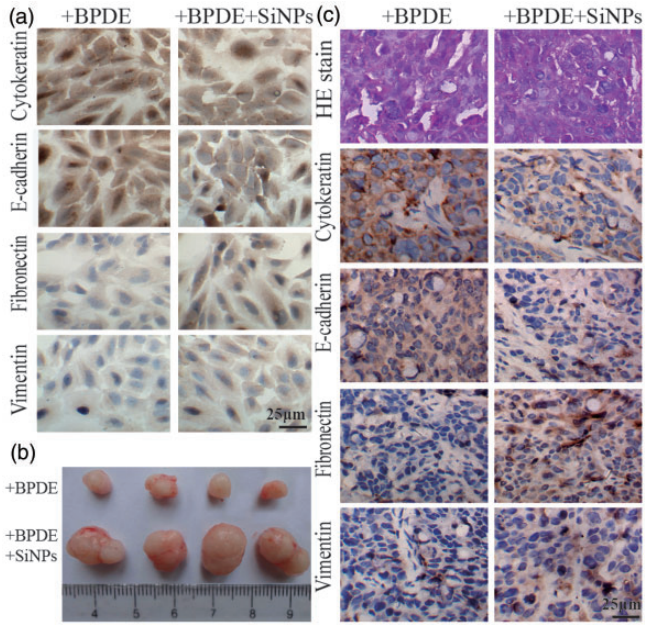

Figure 2. (a) THP-1 and BEAS-2B cells were co-cultured. Cells were treated with BPDE and SiNPs or BPDE alone for 48 hours. Representative immunocytochemical images showing epithelial-mesenchymal transition markers of BEAS-2B cells. (b) THP-1 and BEAS-2B cells were co-cultured. Cells were treated with BPDE ,and SiNPs, or BPDE alone for 48 hours. Xenografting was performed in nude mice. Representative images of xenograft tissue and (c) Hematoxylin–eosin staining of tumor tissue (top panel). Representative images of proteins involved in epithelial-mesenchymal transition analyzed by immunohistochemistry (×400). BPDE: benzo[a]pyrene-7, 8-dihydrodiol-9, 10-epoxide; SiNPs: spherical silica nanoparticles.

SiNPs stimulate secretion of SDF-1α in THP-1 cells

To investigate whether SiNPs play a role in tumorigenesis and EMT of BEAS-2B cells through inflammatory mechanisms, we analyzed cytokines of co-cultures of BEAS-2B and THP-1 cells. SDF-1α expression appeared to be increased after treatment with SiNPs (Figure 3a). To determine whether SDF-1α is secreted by THP-1 cells, THP-1 and BEAS-2B cells were treated with SiNPs. We then tested secretion of SDF-1α in the supernatants of THP-1 and BEAS-2B cells. We found that there were no significant changes in SDF-1α levels in the supernatants of BEAS-2B cell cultures. However, SDF-1α concentrations in THP-1 cell supernatants significantly continuously increased over 36 hours ($p < 0.05$) (Figure 3b). These findings indicated that SDF-1α was mainly secreted by THP-1 in the co-culture system. Furthermore, to study the effect of SiNPs on secretion of SDF-1α, we detected SDF-1α levels with treatment of BPDE with or without SiNPs. We found that secretion of SDF-1α in THP-1 cells was significantly higher with treatment of BPDE compared with controls, but secretion became even higher after being treated with SiNP (both $p < 0.05$) (Figure 3c). SDF-1α mRNA expression levels in THP-1 cells were approximately the same as protein levels, but the fold change was only significant at 36 hours ($p < 0.05$) (Figure 3d).

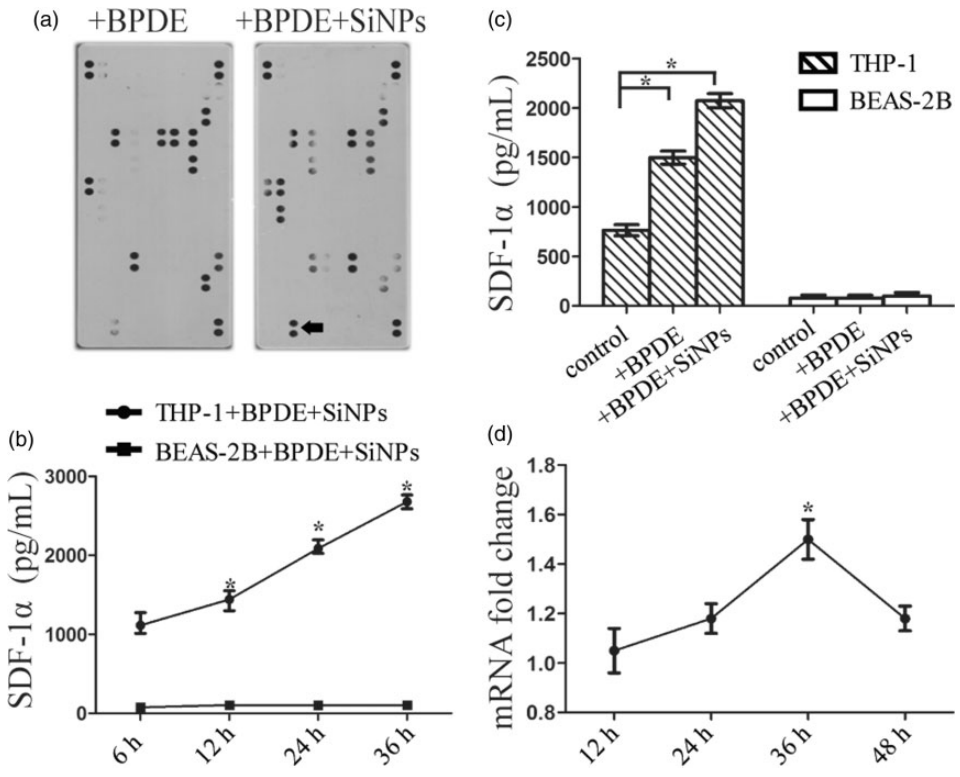

Figure 3. SiNPs stimulate secretion of SDF-1α in THP-1 cells. (a) Secretion of SDF-1α in supernatants of co-cultures of BEAS-2 and THP-1 cells was detected using cytokine chips. SDF-1α is indicted by a black arrow. (b) Changes in SDF-1α levels in the supernatant of THP-1 and BEAS-2B cells at 6 to 36 hours were measured using an enzyme-linked immunosorbent assay. (c) Secretion of SDF-1α in the supernatants of BEAS-2B and THP-1 cells treated by BPDE with or without SiNPs after 24 hours was tested by an enzyme-linked immunosorbent assay and (d) SDF-1α mRNA expression in THP-1cells after treatment with BPDE and SiNPs was determined after 48 hours by real-time polymerase chain reaction. $^*p < 0.05$.
BPDE: benzo[a]pyrene-7, 8-dihydrodiol-9, 10-epoxide; SiNPs: spherical silica nanoparticles; SDF-1α, stromal cell-derived factor-1α.

Neutralization of SDF-1α with a specific antibody inhibits EMT in vivo and in vitro

Neutralization of SDF-1α with a specific antibody resulted in higher cytokeratin and E-cadherin expression and lower fibronectin and vimentin expression in BEAS-2B cells compared with cells with immunoglobulin G treatment (Figure 4a). When BEAS-2B cells treated with a neutralizing antibody against SDF-1α were transplanted subcutaneously in nude mice, expression of proteins involved in EMT in tumor tissues showed similar profiles to those in BEAS-2B cells (Figure 4b).

SDF-1α promotes EMT of BEAS-2B cells via the AKT pathway

SDF-1α can activate the AKT pathway.[15] We found that SiNPs induced p-AKT (ser473) and p-GSK-3β (ser9) expression in BEAS-2B cells and tumor tissue. Neutralizing SDF-1α with a specific antibody resulted in lower p-GSK-3β (ser9) expression compared with GSK-3β

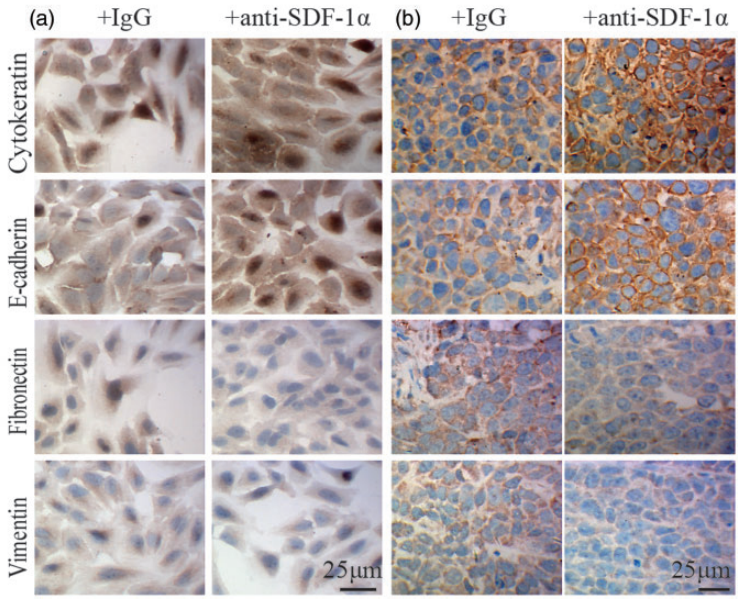

Figure 4. Epithelial-mesenchymal transition was inhibited after neutralizing SDF-1α with antibody in BEAS-2B cells treated with 800 nmol/L benzo[a]pyrene-7, 8-dihydrodiol-9, 10-epoxide and 12.5 μg/mL spherical silica nanoparticles and in tumor tissue (×400). SDF-1α, stromal cell-derived factor-1α.

expression and lower p-AKT-ser473 expression compared with AKT expression (Figure 5a and b). These findings indicated that SDF-1α promoted EMT of BEAS-2B cells via the AKT pathway.

Serum SDF-1α levels in patients with lung cancer from Xuanwei are higher than those in patients with benign pulmonary lesions

SDF-1α levels were significantly lower in patients with lung adenocarcinoma living outside Xuanwei and those with benign pulmonary lesions in Xuanwei than in those with lung adenocarcinoma living in Xuanwei (both $p < 0.05$) (Table 2). There was no significant difference in SDF-1α levels in patients with lung adenocarcinoma in patients outside of Xuanwei when patients were older than 50 years.

Discussion

Many studies have shown that immune infiltrating cells produce and secrete cytokines, which activate protein kinases in metastatic diseases and chronic inflammation to activate many potential developmental processes, including EMT.[16] In chronic inflammation, inflammatory cytokines promote tissue remodeling, angiogenesis, immunosuppression, and growth. This process not only regulates cell phenotypes and functions, but also directly affects malignant transformation of epithelial cells as an initiator, and promotes progression of cancer through chronic inflammation.[17] Crystalline and amorphous silica can induce inflammation, but amorphous silica is considered to have no direct carcinogenicity. Our study showed that SiNPs promoted EMT of BEAS-2B cells by inducing release of SDF-1α from THP-1 cells. These results suggest that

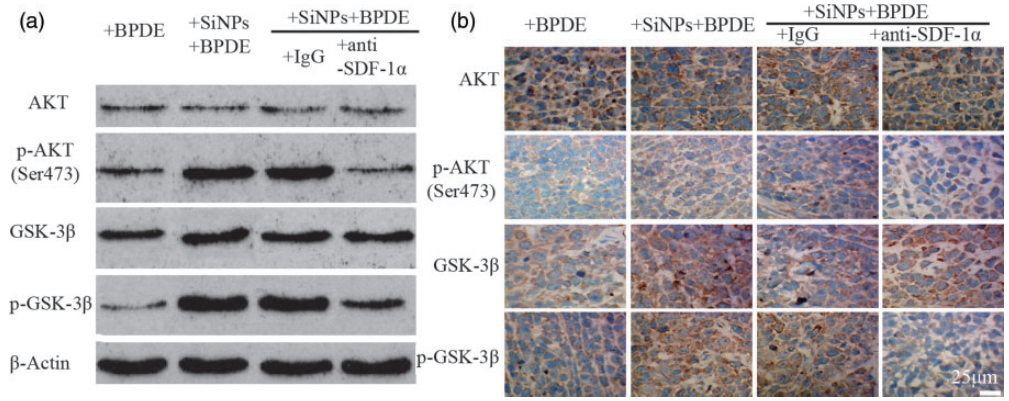

Figure 5. SDF-1α promotes epithelial-mesenchymal transition of BEAS-2B cells via the AKT pathway. Protein expression of AKT, p-AKT, GSK-3β, and p-GSK-3β was detected by western blotting in BEAS-2B cells (a) and by immunohistochemistry in tumor tissue (b) (×400).
BPDE: benzo[a]pyrene-7, 8-dihydrodiol-9, 10-epoxide; SiNPs: spherical silica nanoparticles; SDF-1α, stromal cell-derived factor-1α; GSK-3β, glycogen synthase kinase-3β; p-: phosphorylated.

SiNPs induce an inflammatory response that promotes lung cancer.

A variety of particles have been reported to be toxic to BEAS-2B cells.[18,19] Amorphous silica nanoparticles are small and can easily penetrate cells through the biomembrane, thus causing cell damage and inflammation. Although amorphous silica is cytotoxic, it does not directly cause mutations. However, amorphous silica nanoparticles can increase the incidence of lung cancer *in vivo*.[20] Consistent with our results, amorphous silica nanoparticles can accelerate malignant transformation of cells in the presence of suitable deregulating mutations, which may lead to tumorigenesis.[21] Therefore, amorphous silica nanoparticles may have a role in tumorigenesis of lung cancer.

At present, chronic inflammation is considered to be related to development of tumors. However, rats only show an acute inflammatory response within 8 hours after inhaling amorphous silica nanoparticles. Moreover, after long-term inhalation of SiNPs, most animals only show emphysema and hyperplasia of alveolar cells.[22] In this study, we found that SiNPs promoted EMT of BEAS-2B cells, which is different from the results of these animal experiments. This inconsistency between studies may be due to removal of inhaled silica nanoparticles from the respiratory tract by experimental animals, and thus the duration of inflammation is relatively short. SiNPs act on BEAS-2B cells persistently *in vitro*, eliciting a continuous inflammatory response.

Our findings suggested that SiNPs combined with BPDE promoted EMT by eliciting an inflammatory response. After analysis of a cytokine microarray, we found that SiNPs induced release of SDF-1α levels in the co-culture medium. Further experiments showed that SDF-1α was mainly secreted by THP-1 cells. Combined with BPDE, SiNPs significantly enhanced secretion of SDF-1α. Previous studies have shown that amorphous silica nanoparticles can induce different types of cytokine in different cell lines.[23–25] Our study showed that SiNPs and other types of amorphous silica nanoparticles had different effects on different cytokines, which may be due to the size, concentration, and surface characteristics of the nanoparticles.[26–28] Consequently, different SiNPs may elicit

Table 2. Serum SDF-1α levels as measured by enzyme-linked immunosorbent assay.

		SDF-1α (pg/mL) Median (P25, P75)				
	n	Age < 50 years	n	Age of 50–60 years	n	Age > 60 years
Patients with lung adenocarcinoma in Xuanwei	9	7003.1 (6332, 7782.5)	12	7476.25 (7159.25, 7805.25)	2	7788.5 (7643, 7788.5)
Patients with lung adenocarcinoma outside of Xuanwei in Yunnan	5	5825 (3841, 7311)*	5	5126.2 (3665, 6869)	15	5735.87 (3878, 7429)
Patients with benign pulmonary lesions in Xuanwei	12	1683.2 (1319.25, 1934.75)*	6	1153.3 (619.5, 1797.25)*	4	893.63 (294.87, 1866.5)*

Patients with lung adenocarcinoma outside of Xuanwei and those with benign pulmonary lesions in Xuanwei were compared with those with lung adenocarcinoma in Xuanwei. *$p < 0.05$

different cytokine expression profiles. We found that serum SDF-1α levels in patients with lung cancer were higher than those in patients with benign lesions in Xuanwei, but they were not significantly different from those in lung cancer patients in other districts of Yunnan. This finding may be due to the small number of cases enrolled in this study. In addition, there may be differences between SDF-1α levels in lung tissue and blood samples. Therefore, the relationship between SDF-1α levels and lung adenocarcinoma in Xuanwei requires further study.

SDF-1α (CXCL12) belongs to a class of chemokines that mediate inflammation. SDF-1α is specifically recognized by chemokine receptors 4 and 7.[29] SDF-1α/CXCR4 (CXCR7) plays an important role in tumorigenesis, proliferation, differentiation, and metastasis of various cancers, including breast cancer, colorectal cancer, renal cell carcinoma, ovarian cancer, small cell lung cancer, and others.[30,31] High SDF-1α levels are associated with a shorter survival in patients with esophageal, pancreatic, and lung cancer. However, this finding is the opposite in breast cancer.[32] Recent studies have shown that SDF-1α can enhance angiogenesis and proliferation of small cell lung cancer, and promote invasion and metastasis of lung cancer.[33] Clinical studies have shown that the rate of distant metastasis of patients with non-small cell lung cancer and high CXCR7 expression is significantly higher and the 5-year tumor-free survival rate is significantly lower than those in patients with low CXCR7expression.[34] CXCL12/CXCR4 can activate the AKT pathway. E-cadherin expression is regulated by the AKT pathway, and cytokines are the most important factors that activate AKT signals in tumor cells, such as transforming growth factor-β, epidermal growth factor, hepatocyte growth factor, platelet-derived growth factor, and vascular endothelial growth

factor.[35,36] Dooley and coworkers used transforming growth factor-β to induce EMT in primary mouse liver cells (C57BL/6 mice) and activate AKT signaling.[37] After AKT signal activation by cytokines, the AKT signal upregulated the expression of Snail, Slug, Twist, ZEB, and other nuclear transcription factors, and directly inhibited E-cadherin levels in cells.[38] Our study showed that neutralizing antibody treatment against SDF-1α inhibited activation of the AKT pathway and inhibited EMT of BEAS-2B cells. Therefore, SiNPs promoted EMT of BEAS-2B cells by SDF-1α via the AKT signaling pathway.

In summary, our findings provide evidence that SiNPs combined with BPDE promote EMT of BEAS-2B cells by inducing the release of SDF-1α from THP-1 cells via the AKT pathway. Although direct carcinogenesis of SiNPs cannot be proven currently, this promotes development of tumors combined with BPDE. Therefore, our study provides a theoretical basis for explaining the high incidence of lung cancer in the Xuanwei district of Yunnan, China.

Declaration of conflicting interest

The authors declare that there is no conflict of interest.

Authors' contributions

Chong Guo collected and analyzed/interpreted data (cytokine and chemokine analysis, colony formation assay) and wrote the manuscript. Ding-Yun You conducted statistical analysis of the data. Huan Li collected and analyzed/interpreted data (ELISA, real-time polymerase chain reaction, cell culture). Xiao-Yu Tuo collected and analyzed/interpreted data (animal experiments, cell viability, western blot). Zi-Jie Liu was the principal investigator who conceived and designed the study, performed data analysis and interpretation, and wrote the manuscript.

Funding

This work was supported by the National Natural Science Foundation of China (No. 81460357) and Yunnan Provincial Health and Family Planning Commission (No. 2014NS150, 2018NS0114).

ORCID iD

Zi-Jie Liu http://orcid.org/0000-0002-4734-5554

References

1. Xiao Y, Shao Y, Yu X, et al. The epidemic status and risk factors of lung cancer in Xuanwei City, Yunnan Province, China. *Front Med* 2012; 6: 388–394.
2. Tian L, Dai S, Wang J, et al. Nanoquartz in late permian C1 coal and the high incidence of female lung cancer in the Pearl River Origin area: a retrospective cohort study. *BMC Public Health* 2008; 8: 398.
3. Barone-Adesi F, Chapman RS, Silverman DT, et al. Risk of lung cancer associated with domestic use of coal in Xuanwei, China: retrospective cohort study. *BMJ* 2012; 345: e5414.
4. Yang K, Huang Y, Zhao G, et al. [Expression of PAH-DNA adducts in lung tissues of Xuanwei female lung cancer patients]. *Zhongguo Fei Ai Za Zhi* 2010; 13: 517–521.
5. Vermeulen R, Rothman N and Lan Q. Coal combustion and lung cancer risk in XuanWei: a possible role of silica? *Med Lav* 2011; 102: 362–367.
6. Large DJ, Kelly S, Spiro B, et al. Silica-volatile interaction and the geological cause of the Xuan Wei lung cancer epidemic. *Environ Sci Technol* 2009; 43: 9016–9021.
7. Borm PJ, Tran L and Donaldson K. The carcinogenic action of crystalline silica: a review of the evidence supporting secondary inflammation-driven genotoxicity as a principal mechanism. *Crit Rev Toxicol* 2011; 41: 756–770.
8. Li G, Huang Y, Liu Y, et al. [In vitro toxicity of naturally occurring silica nanoparticles in C1 coal in bronchial epithelial

cells]. *Zhongguo Fei Ai Za Zhi* 2012; 15: 561–568.
9. Grivennikov SI and Karin M. Inflammation and oncogenesis: a vicious connection. *Curr Opin Genet Dev* 2010; 20: 65–71.
10. Zhang Y, Huang W. Transforming growth factor beta1 (TGF-beta1)-stimulated integrin-linked kinase (ILK) regulates migration and epithelial-mesenchymal transition (EMT) of human lens epithelial cells via nuclear factor kappaB (NF-kappaB). *Med Sci Monit* 2018; 24: 7424–430.
11. Wang Z, Sun J, Feng Y, et al. Oncogenic roles and drug target of CXCR4/CXCL12 axis in lung cancer and cancer stem cell. *Tumour Biol* 2016; 37: 8515–8528.
12. De Filippo K and Rankin SM. CXCR4, the master regulator of neutrophil trafficking in homoeostasis and disease. *Eur J Clin Invest* 2018: e12949. doi.org/10.1111/eci.12949
13. Iwagami Y, Casulli S, Nagaoka K, et al. Lambda phage-based vaccine induces antitumor immunity in hepatocellular carcinoma. *Heliyon* 2017; 3: e00407.
14. Seyedabadi S, Saidijam M, Najafi R, et al. Assessment of CEP55, PLK1 and FOXM1 expression in patients with bladder cancer in comparison with healthy individuals. *Cancer Invest* 2018; 36: 407–414.
15. Fu Y, Ma D, Liu Y, et al. Tissue factor pathway inhibitor gene transfer prevents vascular smooth muscle cell proliferation by interfering with the MCP-3/CCR2 pathway. *Lab Invest* 2015; 95: 1246–1257.
16. Dominguez C, David JM and Palena C. Epithelial-mesenchymal transition and inflammation at the site of the primary tumor. *Semin Cancer Biol* 2017; 47: 177–184.
17. Gao D, Vahdat LT, Wong S, et al. Microenvironmental regulation of epithelial-mesenchymal transitions in cancer. *Cancer Res* 2012; 72: 4883–4889.
18. Baroni T, Lilli C, Bellucci C, et al. In vitro cadmium effects on ECM gene expression in human bronchial epithelial cells. *Cytokine* 2015; 72: 9–16.
19. Stabile AM, Marinucci L, Balloni S, et al. Long term effects of cigarette smoke extract or nicotine on nerve growth factor and its receptors in a bronchial epithelial cell line. *Toxicol In Vitro* 2018; 53: 29–36.
20. Morfeld P and Borm P. Re: pulmonary tumor types induced in Wistar rats of the so-called "19-dust study". *Exp Toxicol Pathol* 2007; 58: 407; author reply 9.
21. Fontana C, Kirsch A, Seidel C, et al. In vitro cell transformation induced by synthetic amorphous silica nanoparticles. *Mutat Res* 2017; 823: 22–27.
22. Guichard Y, Maire MA, Sebillaud S, et al. Genotoxicity of synthetic amorphous silica nanoparticles in rats following short-term exposure. Part 2: intratracheal instillation and intravenous injection. *Environ Mol Mutagen* 2015; 56: 228–244.
23. Farcal LR, Uboldi C, Mehn D, et al. Mechanisms of toxicity induced by SiO2 nanoparticles of in vitro human alveolar barrier: effects on cytokine production, oxidative stress induction, surfactant proteins A mRNA expression and nanoparticles uptake. *Nanotoxicology* 2013; 7: 1095–1110.
24. Napierska D, Thomassen LC, Vanaudenaerde B, et al. Cytokine production by co-cultures exposed to monodisperse amorphous silica nanoparticles: the role of size and surface area. *Toxicol Lett* 2012; 211: 98–104.
25. Skuland T, Ovrevik J, Lag M, et al. Silica nanoparticles induce cytokine responses in lung epithelial cells through activation of a p38/TACE/TGF-alpha/EGFR-pathway and NF-kappaBeta signalling. *Toxicol Appl Pharmacol* 2014; 279: 76–86.
26. Mendoza A, Torres-Hernandez JA, Ault JG, et al. Silica nanoparticles induce oxidative stress and inflammation of human peripheral blood mononuclear cells. *Cell Stress Chaperones* 2014; 19: 777–790.
27. Premshekharan G, Nguyen K, Zhang H, et al. Low dose inflammatory potential of silica particles in human-derived THP-1 macrophage cell culture studies - mechanism and effects of particle size and iron. *Chem Biol Interact*. 2017; 272: 160–171.
28. Yang M, Jing L, Wang J, et al. Macrophages participate in local and systemic inflammation induced by amorphous silica nanoparticles through intratracheal instillation. *Int J Nanomedicine* 2016; 11: 6217–6228.
29. Chu T, Shields LBE, Zhang YP, et al. CXCL12/CXCR4/CXCR7 chemokine axis

in the central nervous system: therapeutic targets for remyelination in demyelinating diseases. *Neuroscientist* 2017; 23: 627–648.
30. Liu XQ, Fourel L, Dalonneau F, et al. Biomaterial-enabled delivery of SDF-1alpha at the ventral side of breast cancer cells reveals a crosstalk between cell receptors to promote the invasive phenotype. *Biomaterials* 2017; 127: 61–74.
31. Kajiyama H, Shibata K, Terauchi M, et al. Involvement of SDF-1alpha/CXCR4 axis in the enhanced peritoneal metastasis of epithelial ovarian carcinoma. *Int J Cancer* 2008; 122: 91–99.
32. Samarendra H, Jones K, Petrinic T, et al. A meta-analysis of CXCL12 expression for cancer prognosis. *Br J Cancer* 2017; 117: 124–135.
33. He W, Yang T, Gong XH, et al. Targeting CXC motif chemokine receptor 4 inhibits the proliferation, migration and angiogenesis of lung cancer cells. *Oncol Lett* 2018; 16: 3976–3982.
34. Katsura M, Shoji F, Okamoto T, et al. Correlation between CXCR4/CXCR7/CXCL12 chemokine axis expression and prognosis in lymph-node-positive lung cancer patients. *Cancer Sci* 2018; 109: 154–165.
35. Liu WT, Huang KY, Lu MC, et al. TGF-beta upregulates the translation of USP15 via the PI3K/AKT pathway to promote p53 stability. *Oncogene* 2017; 36: 2715–2723.
36. Popescu AM, Alexandru O, Brindusa C, et al. Targeting the VEGF and PDGF signaling pathway in glioblastoma treatment. *Int J Clin Exp Pathol* 2015; 8: 7825–7837.
37. Dooley S, Meyer C, Liebe R, et.al. Hepatocyte fate upon TGF-β challenge is determined by the matrix environment. *Differentiation* 2015; 89: 105–116.
38. Wang S, Yan Y, Cheng Z, et al. Sotetsuflavone suppresses invasion and metastasis in non-small-cell lung cancer A549 cells by reversing EMT via the TNF-alpha/NF-kappaB and PI3K/AKT signaling pathway. *Cell Death Discov* 2018; 4: 26.